

# Proteasomal selection of multiprotein complexes recruited by LIM homeodomain transcription factors

Cenap Güngör\*, Naoko Taniguchi-Ishigaki\*, Hong Ma\*, Alexander Drung\*, Baris Tursun\*<sup>†</sup>, Heather P. Ostendorff\*<sup>‡</sup>, Michael Bossenz<sup>‡</sup>, Catherina G. Becker<sup>¶</sup>, Thomas Becker<sup>¶</sup>, and Ingolf Bach\*<sup>¶¶</sup>

Programs in \*Gene Function and Expression and <sup>¶</sup>Molecular Medicine, University of Massachusetts Medical School, Worcester, MA 01605; <sup>‡</sup>Center for Molecular Neurobiology (ZMNH), University of Hamburg, D-20251 Hamburg, Germany; and <sup>¶</sup>Centre for Neuroscience Research, Royal (Dick) School of Veterinary Studies, University of Edinburgh, Summerhall, Edinburgh EH9 1QH, United Kingdom

Edited by Michael G. Rosenfeld, University of California at San Diego, La Jolla, CA, and approved July 30, 2007 (received for review April 23, 2007)

Complexes composed of multiple proteins regulate most cellular functions. However, our knowledge about the molecular mechanisms governing the assembly and dynamics of these complexes in cells remains limited. The *in vivo* activity of LIM homeodomain (LIM-HD) proteins, a class of transcription factors that regulates neuronal development, depends on the high-affinity association of their LIM domains with cofactor of LIM homeodomain proteins (LIM-HDs) (CLIM, also known as Ldb or NLI). CLIM cofactors recruit single-stranded DNA-binding protein 1 (SSDP1, also known as SSBP3), and this interaction is important for the activation of the LIM-HD/CLIM protein complex *in vivo*. Here, we identify a cascade of specific protein interactions that protect LIM-HD multiprotein complexes from proteasomal degradation. In this cascade, CLIM stabilizes LIM-HDs, and SSDP1 stabilizes CLIM. Furthermore, we show that stabilizing cofactors prevent binding of ubiquitin ligases to multiple protein interaction domains in LIM-HD recruited protein complexes. Together, our results indicate a combinatorial code that selects specific multiprotein complexes via proteasomal degradation in cells with broad implications for the assembly and specificity of multiprotein complexes.

LIM domain | proteasome | protein complex | protein interaction | ubiquitin

LIM homeodomain proteins (LIM-HDs) play pivotal roles for neuronal development (1, 2). The high affinity interaction between their LIM domains and cofactor of LIM-HD (CLIM) is required for the *in vivo* activity of LIM-HD proteins (3). CLIM proteins interact with single-stranded DNA-binding protein 1 (SSDP1) (4, 5), and this interaction is important for the developmental function of the LIM-HD protein Lhx1 (6).

The 26S proteasome recognizes ubiquitin chains on proteins targeting them for degradation. Several enzymes are involved in the ubiquitination of proteins including ubiquitin ligases (E3), which determine the specificity of this reaction by choosing the substrate to be targeted via protein–protein interaction (7). CLIM cofactors are subject to proteasomal regulation via the ubiquitin ligase RING finger LIM domain-interacting protein (RLIM) (8, 9).

Here we identify a cascade of stabilizing protein interactions involved in the regulation of gene expression with CLIM stabilizing LIM-HD proteins and SSDP1 stabilizing CLIM. Our results show that instability domains on LIM-HD network proteins overlap with protein regions recognized both by destabilizing enzymes/E3s and stabilizing cofactors and that the association of cofactors prevent binding of E3s to their target. Together, these results identify crucial roles of the proteasome in the assembly of LIM-HD complexes.

## Results

**CLIM Cofactors Stabilize LIM-HDs.** Because the proteasome regulates the LIM-HD protein apterous in *Drosophila* (10) we hypothesized that CLIM proteins may exert part of their positive function on LIM-HDs by protecting them from proteasomal

degradation via competing away an unknown destabilizing enzyme(s)/E3(s) from binding to LIM domains.

To test this idea we first examined whether vertebrate LIM-HD proteins are also regulated by the proteasome by treating  $\alpha$ T3 cells, a gonadotrope pituitary cell line that expresses the LIM-HD Lhx3 and CLIM endogenously (8, 11, 12) with proteasome inhibitors. Treatment of  $\alpha$ T3 cells with lactacystin revealed a concentration-dependent accumulation of endogenous Lhx3 and CLIM (Fig. 1A). Because we have previously shown that dominant-negative CLIM (DN-CLIM) containing the LIM interaction domain (LID) is able to prevent the binding of RLIM to LIM domains (8) we investigated whether CLIM stabilizes LIM-HDs. Indeed,  $\alpha$ T3 cells overexpressing CLIM2 or DN-CLIM displayed higher endogenous Lhx3 levels (Fig. 1B). This depended on the presence of the LID, as overexpression of the CLIM mutant CLIM $\Delta$ C lacking the LID led no longer to increased Lhx3 levels. To further investigate the CLIM-mediated accumulation of Lhx3 we compared protein levels with mRNA levels of endogenous Lhx3 of the same DN-CLIM-transfected  $\alpha$ T3 cells. Using Western blots, we detected a 3.2-fold increase in Lhx3 levels in Myc-tagged DN-CLIM-overexpressing cells, whereas quantitative real-time PCR on reverse-transcribed RNA revealed that Lhx3 mRNA levels remained constant (Fig. 1C). These results show that the observed increase in Lhx3 occurred at the protein level, suggesting that by binding to LIM domains CLIM is able to stabilize Lhx3.

Another prediction of our hypothesis is that the LIM domain in LIM-HDs should mediate protein instability. We investigated this by directly comparing protein stabilities of LIM-HDs with and without LIM domains in a developmentally relevant context by using a method that involves the ectopic overexpression of epitope-tagged proteins via mRNA injections in one- to two-cell staged zebrafish embryos and subsequent protein and mRNA detection after various time points (13). We injected mRNAs

Author contributions: C.G. and N.T.-I. contributed equally to this work; C.G., N.T.-I., A.D., B.T., H.P.O., and I.B. designed research; C.G., N.T.-I., H.M., A.D., B.T., H.P.O., M.B., T.B., and I.B. performed research; C.G., N.T.-I., A.D., B.T., H.P.O., C.G.B., T.B., and I.B. analyzed data; and I.B. wrote the paper.

The authors declare no conflict of interest.

This article is a PNAS Direct Submission.

Abbreviations:  $\alpha$ GSU,  $\alpha$  glycoprotein subunit; CLIM, cofactor of LIM homeodomain proteins; DN-CLIM, dominant-negative CLIM; E3, ubiquitin ligase; hpf, hours postfertilization; IP, immunoprecipitation; LCCD, Ldb/CHIP conserved domain; LID, LIM interaction domain; LIM-HD, LIM homeodomain proteins; qRT-PCR, quantitative RT-PCR; RLIM, RING finger LIM domain binding protein; SSDP1, single stranded DNA-binding protein 1; shRNAs, short hairpin RNA.

<sup>†</sup>Present address: Department of Biochemistry and Molecular Biophysics, Columbia University Medical Center, 701 West 168th Street, HHSC 726, New York, NY 10032.

<sup>‡</sup>Present address: Department of Tumor Biology, Massachusetts General Hospital Cancer Center, Charlestown, MA 02129.

<sup>¶¶</sup>To whom correspondence should be addressed. E-mail: ingolf.bach@umassmed.edu.

This article contains supporting information online at [www.pnas.org/cgi/content/full/0703738104/DC1](http://www.pnas.org/cgi/content/full/0703738104/DC1).

© 2007 by The National Academy of Sciences of the USA

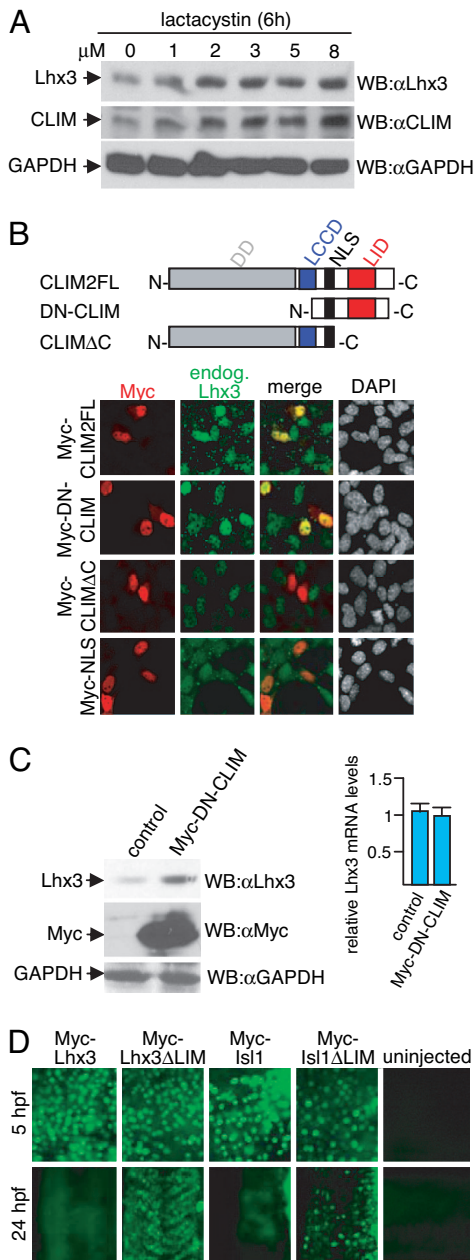


**Fig. 1.** CLIM protects endogenous Lhx3 from proteasomal degradation in  $\alpha$ T3 cells. (A) Cellular levels of Lhx3 and CLIM are regulated by the proteasome. Shown are Western blots of protein extracts that were treated for 6 h with increasing amounts of proteasome inhibitor lactacystin. (B) (Upper) CLIM deletion constructs consisting of CLIM2 full length (CLIM2FL; 1–373), dominant-negative CLIM (DN-CLIM; 245–341), and a C-terminal deletion (CLIM $\Delta$ C; 1–277). DD, dimerization domain; LCCD, Ldb1/Chip conserved domain; NLS, nuclear localization signal; LID, LIM interaction domain. (Lower) Transfection of  $\alpha$ T3 cells with Myc-tagged CLIM expression constructs. Cells are costained with specific Myc (red) and Lhx3 (green) antisera. Note the higher levels of endogenous Lhx3 in cells transfected with Myc-CLIM2FL and Myc-DN-CLIM. (C) (Left) Western blot of protein extracts of cells transfected with Myc-DN-CLIM or the empty vector as control. The same blot was probed with antisera against Lhx3, Myc and GAPDH. Note the higher levels of endogenous Lhx3 in cells transfected with Myc-DN-CLIM. (Right) No change in Lhx3 mRNA levels of the same transfected cells as measured by real-time RT-PCR ( $n = 3$ ; values are mean  $\pm$  SE). (D) The LIM domain mediates instability of LIM-HD proteins. mRNA encoding LIM-HD proteins Lhx3 and Isl1 with or without LIM domains were injected in one- to two-cell-stage zebrafish embryos. Embryos were fixed at 5 and 24 hpf and stained with a monoclonal Myc antibody. At 24 hpf, the focus is on trunk somites. Note that little or no Myc staining is detected in Myc-Lhx3 and Myc-Isl1-injected embryos, whereas  $\Delta$ LIM proteins are readily detectable.

encoding Myc-tagged LIM-HDs Lhx3 or Isl1 with and without LIM domains and examined protein and mRNA at 5 and 24 h postfertilization (hpf). All Myc-fusion proteins were readily detectable at 5 hpf. However, at 24 hpf Myc-LIM-HD fusion proteins could not be detected in full length, whereas the LIM domain-deleted proteins were easily detectable (Fig. 1D). Quantitative RT-PCR (qRT-PCR) experiments confirmed that the stabilities of the full-length and LIM domain-deleted mRNAs were similar, indicating that the observed differences were at the level of protein stability (data not shown). In the zebrafish system, the coexpression of untagged DN-CLIM greatly enhanced Myc-LIM-HD protein levels of Lhx3 and Isl1 at 24 hpf [supporting information (SI) Fig. 5A]. In addition, ectopically overexpressed Myc-DN-CLIM led to higher levels of endogenous LIM-HD proteins of the Isl class in embryonic regions that express low levels of Isl mRNA (SI Fig. 5B) (14). Consistent with a unidirectional protective system, the overexpression of Myc-tagged LIM-HD proteins in  $\alpha$ T3 cells or during zebrafish development did not lead to increased CLIM levels (SI Fig. 5C and D and data not shown). Combined, these results indicate that, by binding to LIM domains, CLIM stabilizes LIM-HDs.

**A Cascade of Stabilizing Protein Interactions in LIM-HD Multiprotein Complexes.** As cellular CLIM levels are subject to proteasomal regulation (Fig. 1A) (8, 9), we mapped protein regions that confer instability during zebrafish development by using Myc-tagged CLIM deletion mutants. We found that N-terminal 277 aa present in Myc-CLIM $\Delta$ C conferred instability at the protein level (SI Fig. 6A). These results are in agreement with our findings that full-length CLIM2 and CLIM $\Delta$ C can interact with the ubiquitin ligase RING finger LIM domain-interacting protein (RLIM, Rnf12) (8) and that in *in vitro* ubiquitination experiments N-terminal, but not C-terminal, sequences of CLIM are polyubiquitinated by RLIM (SI Fig. 6B).

Because we have presented evidence that CLIM cofactors are stabilized during mouse neural tube development (15), we hypothesized that, similar to the protection of LIM-HD by CLIM, binding of proteins to N-terminal CLIM sequences might be responsible for this stabilization. To identify proteins that interact with N-terminal CLIM sequences, we performed a yeast two-hybrid screening of a human brain cDNA library by using CLIM $\Delta$ C as bait and isolated cDNAs encoding different proteins including SSDP1 (data not shown), a known CLIM-interacting protein (4, 5). Because SSDP1 is thought to play a key role in CLIM-mediated activation of LIM-HDs (6), we tested the possibility that SSDP1 stabilizes CLIM. Indeed, overexpressing Myc-SSDP1 in  $\alpha$ T3 cells led to increased endogenous CLIM levels (Fig. 2A). Transfection of N- and C-terminal SSDP1 deletion mutants in  $\alpha$ T3 cells demonstrated that the N-terminal 92 aa (N-SSDP1) containing the CLIM-interaction domain (5) were sufficient for this increase. Zebrafish injections confirmed the stabilization of CLIM by N-SSDP1 (SI Fig. 6C). The fact that SSDP1 stabilizes CLIM and that CLIM stabilizes LIM-HDs suggested that the LIM-HD/CLIM/SSDP1 complex is stabilized via a cascade of protein interactions. This scenario predicts that SSDP1 should also protect LIM-HDs indirectly by protecting CLIM cofactors. Indeed, when cellular SSDP1 levels were knocked down in  $\alpha$ T3 cells via infections with retroviruses containing different SSDP1-short hairpin RNA (shRNAs), cellular CLIM and Lhx3 levels decreased in parallel at the protein, but not at the mRNA level (Fig. 2B). To further examine this protective protein cascade, we transfected SSDP1 proteins fused to GFP and isolated GFP-positive  $\alpha$ T3 cells via FACS. In these experiments, the overexpression of GFP-SSDP1 or GFP-N-SSDP1 fusion proteins led to markedly increased levels of both endogenous CLIM and Lhx3 when compared with GFP-negative cells of the same sorting (Fig. 2C). Again, quantitative RT-PCR experiments using the same cells showed that CLIM and Lhx3

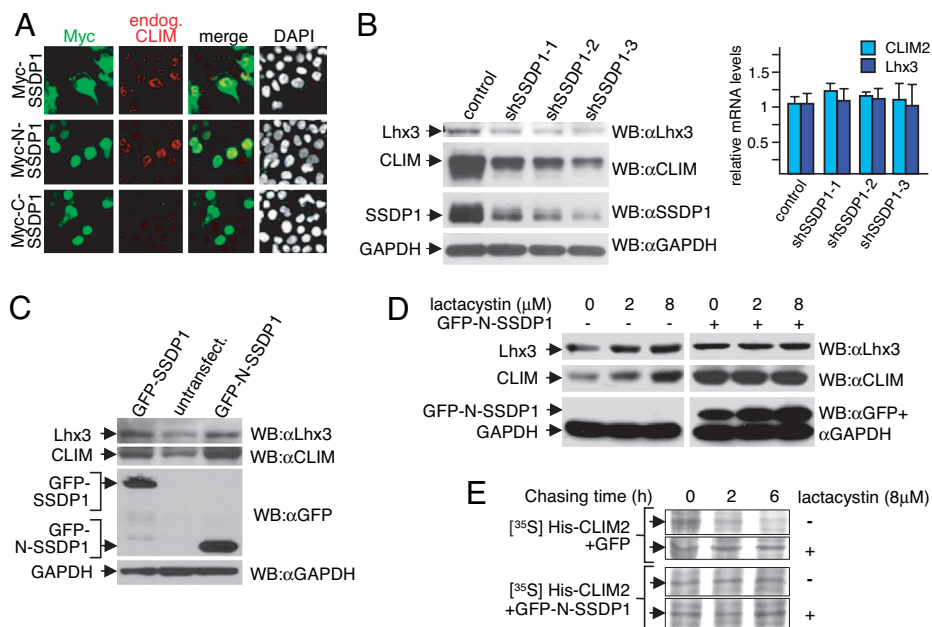


**Fig. 2.** A cascade of protein interactions protects LIM-HD complexes from proteasomal degradation. (A)  $\alpha$ T3 cells were transfected with Myc-SSDP1 expression constructs. Cells are costained with Myc (red) and CLIM (green) antibodies. Note the higher levels of endogenous CLIM in nuclei of cells transfected with Myc-SSDP1 and Myc-N-SSDP1 (1–92) containing the CLIM-interaction domain, but not Myc-C-SSDP1 (90–361). (B) Knock-down of SSDP1 results in decreased levels of endogenous CLIM and Lhx3. SSDP1 levels were knocked-down in  $\alpha$ T3 cells via retroviral infection of three independent mouse shRNAs directed against different regions on SSDP1 or the empty retroviral vector as control. Note that knocking down endogenous SSDP1 levels in  $\alpha$ T3 cells leads to a decrease in endogenous CLIM and Lhx3 protein levels (Left), whereas mRNA levels remain unchanged as measured by qRT-PCR (Right), ( $n = 3$ ; values are mean  $\pm$  SE). (C) Western blot of protein extracts from  $\alpha$ T3 cells transfected with GFP-SSDP1 and GFP-N-SSDP1 expression constructs. GFP-positive cells were isolated via FACS before extract preparation. GFP-negative cells from the same sorting were used as negative control. The same blot was probed with antisera against Lhx3, CLIM, GFP, and GAPDH. Note the higher levels of endogenous CLIM and Lhx3 in cells overexpressing GFP-SSDP1 or GFP-N-SSDP1. (D) SSDP1 protects the Lhx3-CLIM complex from proteasomal degradation.  $\alpha$ T3 cells were transfected with GFP-N-SSDP1 expression construct, and GFP-positive cells were isolated via FACS. Both GFP-positive and GFP-negative cells of the same sorting were cultured overnight. Cells were then treated with indicated concentrations of lactacystin for 6 h before harvesting for Western blotting. The same blot was probed with antisera against Lhx3, CLIM, and GFP/GAPDH. Note that Lhx3 and CLIM protein levels in GFP-N-SSDP1-expressing cells are no longer sensitive to lactacystin. (E) SSDP1 increases the half-life of CLIM. His-tagged CLIM2 was coexpressed in HEK293T cells with GFP or GFP-N-SSDP1 and total cellular proteins were labeled with [ $^{35}$ S]methionine for 1 h, followed by washings and chasing in normal medium for indicated time periods in the presence or absence of lactacystin.

mRNA levels remained essentially unchanged (data not shown). We next investigated whether these increases in cellular CLIM and Lhx3 concentrations occurred at the level of proteasomal protection by treating GFP or GFP-N-SSDP1 expressing  $\alpha$ T3 cells with proteasome inhibitor lactacystin. Whereas the endogenous CLIM and Lhx3 levels in GFP-negative cells increased upon lactacystin treatment, cellular levels of both proteins remained insensitive to proteasome inhibitor in GFP-N-SSDP1-expressing cells (Fig. 2D). An increase in GFP-N-SSDP1 levels in these experiments and endogenous SSDP1 levels (SI Fig. 7A) upon lactacystin treatment suggested that SSDP1 is also regulated by the proteasome. To distinguish between protein stability and steady-state protein levels we performed a pulse-chase experiment labeling total cellular protein with [ $^{35}$ S]methionine in HEK293 cells cotransfected with His-CLIM2 and GFP-N-SSDP1. These experiments revealed an N-SSDP1-mediated increase in CLIM stability via protection from proteasomal targeting (Fig. 2E). The CLIM-SSDP1 protective system was also unidirectional as overexpression of CLIM did not lead to increased SSDP1 levels in  $\alpha$ T3 cells (data not shown). Combined, these results demonstrate a hierarchical cascade of protein interactions recruited by LIM-HD transcription factors that protect against proteasomal degradation at multiple levels.

**The LCCD Region in CLIM Mediates Instability and Interacts with RLIM and SSDP1.** The SSDP1 interaction domain on CLIM (amino acid 214–223) is embedded in a larger conserved region of 50 aa termed the Ldb/Chip conserved domain (LCCD; amino acid

201–250) (5). To further substantiate that binding of SSDP1 protects CLIM from proteasomal degradation, we tested whether the LCCD functions as an instability domain in zebrafish. Whereas the 6xMyc-NLS protein was readily detectable at 5 and 24 hpf (13, 14), we detected 6xMyc-LCCD at 5 hpf, but no longer at 24 hpf (Fig. 3A). Because qRT-PCR experiments showed similar levels for mRNAs encoding the 6xMyc-tag and the 6xMyc-LCCD (data not shown), these results identify the LCCD as a domain conferring protein instability. Because RLIM polyubiquitinates and targets CLIM for proteasomal degradation, we tested whether the LCCD region mediates interaction with RLIM. Indeed, in GST pull-downs, the Myc-LCCD robustly interacted with RLIM (Fig. 3B). Moreover, in coimmunoprecipitations (co-IPs) using transfected  $\alpha$ T3 cell extracts, Myc-LCCD interacted with both endogenous RLIM and SSDP1 (Fig. 3C). Thus, the LCCD region of CLIM interacts with RLIM and SSDP1. As SSDP1 protects CLIM from proteasomal degradation we examined the involved mechanisms. In *in vitro* ubiquitinations using  $^{35}$ S-CLIM $\Delta$ C as substrate and bacterially expressed GST-RLIM, the presence of GST-N-SSDP1 partially inhibited ubiquitinations of CLIM $\Delta$ C (Fig. 4A). GST pull-down experiments using  $^{35}$ S-labeled Myc-LCCD alone or cotranslated with Myc-N-SSDP1 showed that the presence of N-SSDP1 inhibits the LCCD-RLIM interaction (Fig. 4B). Furthermore, in cells the interaction of endogenous RLIM with Myc-LCCD is inhibited in the presence of GFP-N-SSDP1 in co-IPs (Fig. 4C). Thus, the LCCD interacts with both RLIM and SSDP1 and the association of SSDP1 inhibits RLIM from binding and ubiquitinating CLIM.

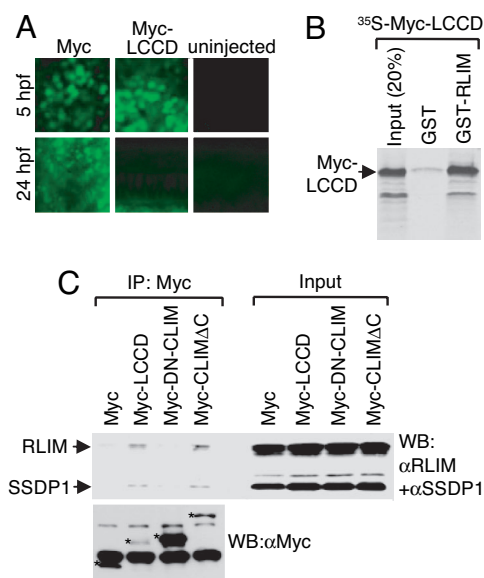


**Fig. 3.** The LCCD region interacts with SSDP1 and RLIM and mediates instability. (A) The LCCD domain functions as an instability domain. mRNA encoding Myc-LCCD was injected in zebrafish embryos. Embryos were fixed at 5 and 24 hpf and stained with a monoclonal Myc antibody. Note that little or no Myc staining is detected in 24 hpf embryos of Myc-LCCD-injected animals, whereas Myc-NLS control proteins are readily detectable. (B) The LCCD region interacts directly with RLIM *in vitro*. Shown is GST pull-down using GST-RLIM and [<sup>35</sup>S]Myc-LCCD. (C) The LCCD interacts with RLIM and SSDP1 in cells. Co-IP of SSDP1 and RLIM from  $\alpha$ T3 cells transfected with Myc-LCCD. (Upper) Western blot of Myc IPs (Left) and 100% input control (Right) using antibodies directed against RLIM and SSDP1 (10% gel). (Lower) To visualize Myc-proteins, an aliquot of the same Myc-IPs was run on a 15% gel in parallel. Myc proteins are indicated by asterisks. Lower Myc-LCCD and Myc-CLIM $\Delta$ C protein levels probably reflect their instability in cells. Bands not marked with asterisks are unpecific.

We next investigated whether the SSDP1/CLIM/Lhx3 protein cascade is of functional relevance for LIM-HD complexes on the  $\alpha$ GSU promoter, because we have previously shown that this promoter is regulated by the LIM-HD Lhx3 in conjunction with CLIM in  $\alpha$ T3 cells (8, 16). In agreement with these data and the known association of SSDP1 with CLIM cofactors (4, 5), we detected SSDP1 on the active  $\alpha$ GSU promoter in  $\alpha$ T3 cells and found decreased promoter occupancy of CLIM and Lhx3 when SSDP1 levels were knocked down using ChIP/real-time PCR (SI Fig. 7 B and C). Conversely, the overexpression of SSDP1 led to increased occupation of Lhx3 and CLIM (data not shown). To examine whether these changes in promoter occupation had an effect on endogenous  $\alpha$ GSU expression we tested mRNA and protein levels in  $\alpha$ T3 cells mostly depleted of SSDP1. Indeed,  $\alpha$ T3 cells in which SSDP1 levels were knocked down via retroviral shRNA infection expressed markedly lower levels of mRNAs encoding  $\alpha$ GSU as well as  $\alpha$ GSU protein (Fig. 4D) when compared with control-infected cells. These results show that the disturbance of the SSDP1/CLIM/Lhx3 protein cascade directly influences gene expression of endogenous LIM-HD target genes.

## Discussion

We have shown that LIM-HDs are regulated by the proteasome and that CLIM stabilizes LIM-HDs by binding to LIM domains. These data combined with our findings that the LIM domains of several LIM proteins have been shown to bind ubiquitin ligases (17–20) and that the ubiquitin ligase RLIM does not mediate ubiquitination/degradation of LIM-HDs (8, 9), strongly suggest that CLIM inhibits binding of an as-yet-unknown E3 ligase to LIM-HDs. In addition, the fact that the LIM-interaction domain

LID in CLIM is sufficient to stabilize LIM-HDs, that CLIM cofactors bind to LIM domains with high affinity (3), and that the LID of CLIM prevents ubiquitination of LIM-only protein LMO2 (8), strongly argues that LIM-HD stabilization via CLIM occurs at the level of competition with destabilizing enzymes/E3s for binding to LIM domains. However, at present no E3 enzyme for LIM-HDs has been identified, and we cannot rule out the possibility that a change in LIM-HD protein conformation induced by CLIM binding may contribute to the protective effect. Thus, these results pinpoint the LIM domain in LIM-HDs as a critical instability domain that is stabilized via CLIM interaction, providing a molecular mechanism both for previously observed negative functions of LIM domains (21) and positive functions of the LIM-HD-CLIM interaction (16, 22). However, because in zebrafish experiments LIM domain-deleted proteins appear less stable when compared with NLS-Myc (data not shown), it is likely that additional domains that confer instability exist in LIM-HD proteins.

In addition to LIM domains, we have shown that the LCCD in CLIM provides instability by recruiting the E3 ligase RLIM and that SSDP1 prevents the RLIM-LCCD interaction, thereby stabilizing CLIM. Again, the inhibition of RLIM by SSDP1 may be at the level of competition for binding and/or an induced change in protein conformation. Our findings suggest that conserved protein regions such as the LIM domain and the LCCD are protein regions that integrate negative signals (degradation) with positive signals (protective cofactor interactions). This interpretation is consistent with previously published results that show the competition for binding sites in a protein network comprising p53, an elongin C-containing E3 ligase and van Hippel Lindau protein (pVHL) (23), suggesting that this theme of inhibition of E3 ligases by cofactor binding may be a more widely applied mechanism for the regulation of protein stability. Our data are in full agreement with results published around the time this manuscript was submitted, which reported a cascade of stabilizing protein interactions involving transcription factors GATA-1, SCL (Tal-1), E47 and LIM-only protein 2 (LMO2), CLIM, and SSBP2 during erythropoiesis (24).

Although many cofactors are widely expressed and potentially form complexes with a variety of different classes of transcription factors, specific transcription factors can use distinct combinations of cofactors in specific cell types or promoter contexts (25, 26), showing that the cell nevertheless achieves specificity in protein complex formation. Our results indicate that the proteasome targets LIM network proteins for degradation that are not associated with protecting cofactors. The findings that (i) stabilizing cofactors and destabilizing enzymes bind to protein regions that confer instability and that (ii) cofactor binding inhibits E3 ligases indicates a combinatorial code consisting of protecting cofactors and E3 enzymes, which together select specific multiprotein complexes via proteasomal degradation in cells (see also Fig. 4E). As it is generally accepted that each cell type expresses a specific set (or levels) of regulatory proteins such as protecting cofactors and destabilizing enzymes/ubiquitin ligases, it is tempting to speculate that the proteasome will select different complexes in different cell types, thereby contributing to the formation of cell type-specific complexes. Because most cellular processes, including transcription, are regulated by large complexes consisting of many different proteins, many of which are widely expressed (27–29), our results are likely to impact more generally the dynamics and specificity of cellular protein complexes.

## Methods

**Antibodies and Plasmids.** Antisera and monoclonal antibodies used in this study were previously described CLIM (8), Lhx3 (15), or purchased: Isl (Developmental Studies Hybridoma Bank, University of Iowa, Iowa City, IA), SSDP1 (Abnova, Taipei City, Taiwan), Myc (Santa Cruz Biochemicals, Santa Cruz, CA), GAPDH (Chemicon, Temecula, CA),  $\alpha$ -tubulin

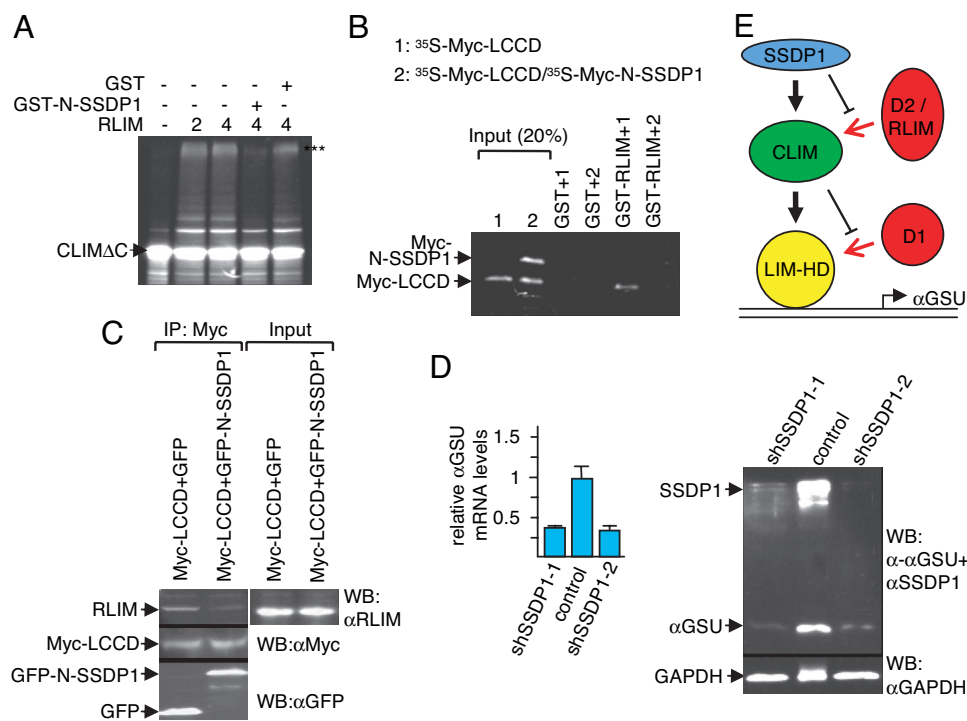


**Fig. 4.** SSDP1 inhibits binding of RLIM to CLIM and regulates Lhx3 target gene expression. (A) *In vitro* ubiquitination experiment using  $^{35}\text{S}$ -labeled CLIM $\Delta$ C, RLIM as E3, and UbcH5 as E2 enzyme in the presence of GST-N-SSDP1 or GST alone. Arrows point at unmodified CLIM proteins. Polyubiquitinated proteins are indicated by three asterisks (\*\*\*) Note the partial inhibition of CLIM $\Delta$ C ubiquitination by N-SSDP1. (B) N-SSDP1 inhibits binding of RLIM to the LCCD. Shown is the GST pull-down using GST-RLIM and  $^{35}\text{S}$ -Myc-LCCD (1) or Myc-LCCD cotranslated with Myc-N-SSDP1 ( $^{35}\text{S}$ -Myc-LCCD/ $^{35}\text{S}$ -Myc-N-SSDP1) (2). (C) Co-IP of endogenous RLIM in cells cotransfected with Myc-LCCD and GFP-N-SSDP1. Note the decreased RLIM precipitation in the presence of N-SSDP1. (D) Down-regulation of SSDP1 results in lower levels of  $\alpha$ GSU mRNA and protein. (Left) SSDP1 levels were knocked-down in  $\alpha$ T3 cells via retroviral infection of mouse shRNAs (shSSDP1-1, -2) or the empty retroviral vector. mRNA encoding  $\alpha$ GSU was measured by qRT-PCR ( $n = 3$ ; values are mean  $\pm$  SE). (Right) Western blot of the same shRNA-treated cells. Note that knocking down endogenous SSDP1 levels leads to a significant decrease in endogenous  $\alpha$ GSU levels at the mRNA and protein levels. (E) Shown is a model of a cascade of protein interactions that protects LIM-HDs from proteasomal degradation. Via binding to LIM domains, a destabilizing enzyme (D1, red) targets LIM-HDs (yellow) for degradation. In the presence of CLIM (green), the binding of D1 to LIM domains is inhibited, resulting in stabilization of LIM-HDs. CLIM is targeted by another destabilizing enzyme(s) (D2/RLIM) for ubiquitination/degradation. The presence of SSDP1 (blue) prevents binding of D2/RLIM to CLIM thereby protecting the LIM-HD/CLIM protein complex.

(Sigma, St. Louis, MO),  $\alpha$ GSU (National Hormone and Pituitary Program, Torrance, CA). Expression plasmids of proteins used in this work were as follows: CLIM $\Delta$ C, DN-CLIM, CLIM1, CLIM2, His-CLIM2, Lhx3, Lhx3 $\Delta$ LIM, RLIM, Lmx1, Lhx1, Lhx2, Isl1, and Isl1 $\Delta$ LIM (8, 12, 16, 17). For the NLS-6xMyc-LCCD expression plasmid, a fragment encoding amino acids 201–249 of CLIM2 containing the LCCD and SSDP1 interaction domain of CLIM2 was inserted in the pCS2NLS-MT vector. For expression of SSDP1 (full length), N-SSDP1 (1–92) and C-SSDP1 (90–361), were inserted in pCS2, pCS2-MT, and pCS2-NLS-MT. Expression plasmids for GFP-SSDP1 and GFP-N-SSDP1 fusion proteins were generated by using the pEGFP-C1.

**Cell Culture, Transient Transfections, Immunocytochemistry, and Retroviral Infections.** Gonadotrope pituitary  $\alpha$ T3 cells were cultured as described in ref. 11. Transient transfections and cotransfections were carried out using a Superfect transfection kit (Qiagen, Valencia, CA) or the calcium phosphate method as described in ref. 23. Immunocytochemical stainings and costainings of cells were performed as reported in ref. 8. The experiments were analyzed and images were taken on a Leica (Deerfield, IL) confocal microscope. SSDP1 shRNAs (Open Biosystems, Huntsville, AL) in the retroviral vector pSM2 allowed the preparation of retrovirus by cotransfection with pEcopack.  $\alpha$ T3 cells were infected as described in ref. 30, and infected cells were selected in 0.6  $\mu\text{g}/\text{ml}$  puromycin.

**Western Blots, Quantitative RT-PCR, Half-Life Experiments, and Yeast-Two-Hybrid Screening.** Protein levels of transfected cells were monitored by Western blots as described in ref. 8 by using CLIM,

Lhx3, SSDP1, GAPDH, or  $\alpha$ -tubulin antisera. For the preparation of cell extracts, we used the PARIS kit (Ambion, Austin, TX) that allows parallel preparation of protein as well as mRNA from the same cells. mRNA levels were quantified using quantitative RT-PCR as described in ref. 31. In brief, 1  $\mu\text{g}$  of total RNA was reverse transcribed with Oligo-dT primer. For the thermal cycle reaction, the i-Cycler system (BioRad, Hercules, CA) was used at 50°C for 2 min, 95°C for 10 min, then 40 cycles at 95°C for 15 s, and at 60°C for 1 min. All experiments were performed in triplicate.  $\beta$ -actin served as an internal standard control. The primer sequence for the examined genes were as follows:  $\beta$ -actin forward, 5'-GCAAGTGCTTCTAGCGGAC-3';  $\beta$ -actin reverse, 5'-AAGAAAGGGTGTAAAACGCAGC-3'; CLIM2 forward, 5'-AACTCCCATGTACCCACCTACA-3'; CLIM2 reverse, 5'-GCAGAAAGTGATGGTCAGCATG-3'; Lhx3 forward, 5'-CGGGCTAAGGAAAAGAGACTG-3'; Lhx3 reverse, 5'-CTGCTGTACAGGCCATTAGCA-3';  $\alpha$ GSU forward, 5'-TCCAGAGACATTGTTCCCTCA-3';  $\alpha$ GSU reverse, 5'-ATGCAGGAACATGGACAGCATG-3'. The threshold cycle of each gene was determined as the number of PCR cycles at which the increase in reporter fluorescence was 10 times above a baseline signal. Log starting quantity gave the weight of the gene contained in each sample. The weight ratio of the target gene to  $\beta$ -actin gave the standardized expression level. For qRT-PCR from zebrafish, the primer sequences for amplifying the Myc-tag in pCS2-MT and  $\beta$ -actin have been reported in ref. 13. RNA from uninjected animals served as a negative control.

Half-life experiments were performed as described in ref. 20, with the modification that His-tagged CLIM2 was used and purified via Ni-NTA agarose (Qiagen).

The Matchmaker Two-Hybrid System 3 (Clontech, Mountain View, CA) was used to screen a mouse fetal brain cDNA library in pACT2 (GAL4-AD fusion). The bait plasmid was CLIMΔC in pGBKT7. Interacting clones were identified by the ability to grow on minimal SD agar medium lacking tryptophan, leucine, histidine, and adenine (Clontech). Prey plasmids were recovered and retransformed into AH109 together with the bait to verify interactions by β-galactosidase filter lift assays.

**Zebrafish mRNA Injections, GST Pull-Down, *in vitro* Ubiquitination, and ChIP Assays.** All mRNAs encoding LIM-HD, CLIM, and SSDP1 proteins were produced from pCS2-MT plasmids for Myc-tagged

and pCS2 plasmids for untagged proteins by using the mMessage mMachinE kit (Ambion) and Sp6 RNA polymerase. Zebrafish microinjections were carried out as described in ref. 14. Animals were allowed to develop to 5 or 24 hpf, at which point they were processed for immunohistochemistry, RT-PCR, or Western blot analyses. All injections were repeated at least three times. Survival rates between injected and uninjected embryos were indistinguishable. GST pull-downs, *in vitro* ubiquitinations, and ChIP assays were performed as described in refs. 8 and 12.

We thank M. Hochstrasser, A. Israel, P. Kaufman, C. Peterson, and P. Zamore for helpful discussion and advice and C. Carriere for reading the manuscript. I.B. was supported by grants from the Deutsche Forschungsgemeinschaft, Wings for Life, and the Worcester Foundation for Biomedical Research.

1. Bach I (2000) *Mech Dev* 91:5–17.
2. Hobert O, Westphal H (2000) *Trends Genet* 16:75–83.
3. Matthews JM, Visvader JE (2003) *EMBO Rep* 4:1132–1137.
4. Chen L, Segal D, Hukriede NA, Podtelejnikov AV, Bayarsaihan D, Kennison JA, Ogryzko VV, Dawid IB, Westphal H (2002) *Proc Natl Acad Sci USA* 99:14320–14325.
5. van Meyel DJ, Thomas JB, Agulnick AD (2003) *Development (Cambridge, UK)* 130:1915–1925.
6. Nishioka N, Nagano S, Nakayama R, Kiyonari H, Ijiri T, Taniguchi K, Shawlot W, Hayashizaki Y, Westphal H, Behringer RR, et al. (2005) *Development (Cambridge, UK)* 132:2535–2546.
7. Pickart CM (2001) *Annu Rev Biochem* 70:503–533.
8. Ostendorff HP, Peirano RI, Peters MA, Schlüter A, Bossenz M, Scheffner M, Bach I (2002) *Nature* 416:99–103.
9. Hiratani I, Yamamoto N, Mochizuki T, Ohmori SY, Taira M (2003) *Development (Cambridge, UK)* 130:4161–4175.
10. Weihe U, Milan M, Cohen SM (2001) *Development (Cambridge, UK)* 128:4615–4622.
11. Windle JJ, Weiner RI, Mellon PL (1990) *Mol Endocrinol* 4:597–603.
12. Bach I, Rhodes SJ, Pearse RV, Heinzel T, Gloss B, Scully KM, Sawchenko PE, Rosenfeld MG (1995) *Proc Natl Acad Sci USA* 92:2720–2724.
13. Becker T, Bossenz M, Tursun B, Schlüter A, Peters MA, Becker CG, Ostendorff HP, Bach I (2003) *Methods Cell Sci* 25:85–89.
14. Becker T, Ostendorff HP, Bossenz M, Schlüter A, Becker C, Peirano RI, Bach I (2002) *Mech Dev* 117:75–85.
15. Ostendorff HP, Tursun B, Cornils K, Schlüter A, Drung A, Gungor C, Bach I (2006) *Dev Dyn* 235:786–791.
16. Bach I, Carriere C, Ostendorff HP, Andersen B, Rosenfeld MG (1997) *Genes Dev* 11:1370–1380.
17. Bach I, Rodriguez-Esteban C, Carriere C, Bhushan A, Kronen A, Rose DW, Glass CK, Andersen B, Izpisua Belmonte JC, Rosenfeld MG (1999) *Nat Genet* 22:394–399.
18. Didier C, Broday L, Bhoumik A, Israeli S, Takahashi S, Nakayama K, Thomas SM, Turner CE, Henderson S, Sabe H, et al. (2003) *Mol Cell Biol* 23:5331–5345.
19. Broday L, Kolotuev I, Didier C, Bhoumik A, Podbilewicz B, Ronai Z (2004) *J Cell Biol* 165:857–867.
20. Tursun B, Schlüter A, Peters MA, Viehweger B, Ostendorff HP, Soosairajah J, Drung A, Bossenz M, Johnsen SA, Schweizer M, et al. (2005) *Genes Dev* 19:2307–2319.
21. Taira M, Otani H, Saint-Jeannet JP, Dawid IB (1994) *Nature* 372:677–679.
22. Thaler JP, Lee SK, Jurata LW, Gill GN, Pfaff SL (2002) *Cell* 110:237–249.
23. Roe JS, Kim H, Lee SM, Kim ST, Cho EJ, Youn HD (2006) *Mol Cell* 22:395–405.
24. Xu Z, Meng X, Cai Y, Liang H, Nagarajan L, Brandt SJ (2007) *Genes Dev* 21:942–955.
25. Hermanson O, Glass CK, Rosenfeld MG (2002) *Trends Endocrinol Metab* 13:55–60.
26. Rosenfeld MG, Lunyak VV, Glass CK (2006) *Genes Dev* 20:1405–1428.
27. Naar AM, Lemon BD, Tjian R (2001) *Annu Rev Biochem* 70:475–501.
28. Glass CK, Rosenfeld MG (2000) *Genes Dev* 14:121–141.
29. Bach I, Ostendorff HP (2003) *Trends Biochem Sci* 28:189–195.
30. Pear WS, Nolan GP, Scott ML, Baltimore D (1993) *Proc Natl Acad Sci USA* 90:8392–8396.
31. Lipson KL, Fonseca SG, Ishigaki S, Nguyen LX, Foss E, Bortell R, Rossini AA, Urano F (2006) *Cell Metab* 4:245–254.